AUGUST 01 2025

Experimental implementation of an actively controlled tuned vibration absorber using piezoelectric actuators

Beth Austin (10); Jordan Cheer (10)



Proc. Mtgs. Acoust. 57, 065001 (2025) https://doi.org/10.1121/2.0002056





Articles You May Be Interested In

Experimental validation of a multi-material Acoustic Black Hole

Proc. Mtgs. Acoust. (May 2024)

Active vibration and structural acoustic control of shape memory alloy hybrid composites: Experimental results

J. Acoust. Soc. Am. (December 1990)

Experimental realization of a nonlinear acoustic lens with a tunable focus

Appl. Phys. Lett. (January 2014)





Volume 57

http://acousticalsociety.org/



NOVEM2025

NOise and Vibration Emerging Methods

Garmisch-Partenkirchen, Germany
6-8 May 2025

Structural Acoustics and Vibration: Noise and Vibration Control

Experimental implementation of an actively controlled tuned vibration absorber using piezoelectric actuators

Beth Austin and Jordan Cheer

Institute of Sound and Vibration Research, University of Southampton, Southampton, Hampshire, SO17 1BJ, UNITED KINGDOM; b.austin@soton.ac.uk; j.cheer@soton.ac.uk

Tuned vibration absorbers (TVAs) are known to provide effective vibration control at their specific tuning frequency. They can effectively dissipate vibration energy from the host structure, making them useful for the control of both time invariant tonal excitation and structural resonances. However, they are ineffective away from their tuning frequency, making them unsuitable for applications where broadband vibration control is required or where there is significant variance in the system dynamics or the vibration spectrum. By incorporating some form of actuation and sensing into a TVA, active control can be used to vary the response of a TVA after production, tuning the TVA dynamics to the potential time varying application requirements. This paper explores the tunability of a specific TVA design, where the spring elements of the TVA are actuated using piezoelectric patch actuators. Previous work has studied the theoretical limits of controlling the dynamics of this TVA design using feedback control strategies. The work presented in this paper extends this to an experimental implementation of active control on the proposed TVA design using commercially available piezoelectric actuators and sensors to establish the practical limits on actively tuning the considered TVA design.



1. INTRODUCTION

Tuned Vibration Absorbers (TVAs) are a well established method of controlling vibration over narrow frequency bands. For example, they can effectively control vibration associated with structural resonances or narrowband driven responses.¹ Arrays of TVA-like resonators are also increasingly being used to form metamaterials, which can potentially achieve high levels of control over wider frequency bands depending on the tuning of the constituent TVAs.^{2,3} Metamaterials are broadly defined by their ability to achieve unusual effective material properties that are not typically found in conventional materials, such as negative stiffness or mass. However, in the context of vibration control, they may also be characterised by their ability to achieve high levels of control performance with features that are small compared to the wavelength of vibration. Metamaterials generally consist of an array of sub-structures, known as unit cells, that interact with waves at a sub-wavelength scale. These metamaterial treatments typically require a smaller overall volume of material compared to realising the same performance with a conventional bulk material and, therefore, they are becoming increasingly useful when realising lightweight structures.

When realising a metamaterial for practical application, it is necessary to consider uncertainty in both the manufacturing of the unit cells and the host structure itself, and variation in the excitation of the host structure. For a metamaterial realised using an array of TVAs, the performance will be dependent on the resonance frequencies of the realised TVAs. If these vary in an unmodelled way due to manufacturing, for example, then this may inadvertently limit the control performance. This has been addressed in previous work by optimising the design of a unit cell consisting of multiple resonators to be robust to uncertainties in the resonance frequencies of the realised resonators.⁴ Similarly, the unit cells for resonator-based metamaterials have been optimally designed to be robust to variations in the response of the structure to which they are attached by either distributing the tuning frequencies,^{3,4} or by adapting the tuning frequencies through the realisation of a semi-active resonator, or TVA.⁵ In the case of realising a robust passive TVA-based metamaterial, as in Singleton et al.,³ the design is fixed at the manufacturing stage and so a trade-off between performance and robustness must be selected at this point. In the case of the semi-active TVA case, however, a greater flexibility is provided in that the tuning frequencies can be adapted over time to enable the resonance frequencies to be adapted to provide the maximum performance for the current system response. However, by moving to a fully active TVA approach, it is possible to vary additional characteristics of the TVA response, including frequency and damping, and potentially achieve this in a more dynamic way to manage variations in both the response of the TVA and the structure to which it is applied.

This paper extends to an experimental implementation a previous simulation study into the potential of actively tuning the response of a TVA design,⁶ which was previously proposed in Singleton et al.,³ by actuating via a feedback control strategy the springs of the resonator-based TVA. Section 2 discusses the design of the TVA and describes the active control strategy. Section 3 describes the experimental methodology and Section 4 presents the experimental results, showing both the response of the implemented TVA and the limits on its tunability via three different feedback control strategies.

2. ACTIVE TUNED VIBRATION ABSORBER

The TVA used in this work is based on the passive design proposed in, ⁷ and the initial simulation based study into the active TVA reported in. ⁶ The TVA is designed to act as a single degree of freedom mass-spring-damper, and its response can therefore be described by the equation of motion, expressed as

$$m\ddot{x} + c\dot{x} + kx = F,\tag{1}$$

where m is the moving mass, c is the damping factor, k is the spring stiffness, F is the force applied to the mass, and x is the relative displacement between the mass and the base, $x = x_m - d$. A diagram of the

basic mass-spring-damper is shown in Figure 1 and a diagram showing the assumed physical realisation that has been previously designed³ to achieve this mass-spring-damper response is shown in Figure 2. This TVA design consists of three cantilever beams oriented at 120° to each other to minimise the lateral motion of the mass ring which they support; the cantilever beams are supported by pillars, which raise the mass ring away from the structure to which the TVA is applied, and these pillars are in turn connected via a base ring to the structure being controlled. The three beams form the spring element of the mass-spring-damper and also provide the damping, while the mass ring forms the moving mass. In the proposed active TVA realisation, the springs are each actuated using piezoelectric elements, which can be driven variously to modify the response of the TVA. Passively, without the piezoelectric actuators attached, each beam would provide an equivalent spring stiffness, k, given by

 $k = \frac{3EI}{L^3},\tag{2}$

where E is the Young's modulus of the beam material, I is the second moment of inertia of the beam, and L is the length of the beam. The three beams act as springs in parallel, thus providing a total spring stiffness three times larger than this. As such, the expected natural frequency of the TVA, f_0 , can be expressed as

$$f_0 = \frac{1}{2\pi} \sqrt{\frac{9EI}{mL^3}},\tag{3}$$

where m is the moving mass provided by the mass ring in this instance. This simple relationship offers an initial estimation of the tuning frequency that a simple TVA design can achieve passively, although the addition of the undriven piezoelectric actuators will also change the properties of the beams, mostly via a stiffening effect.

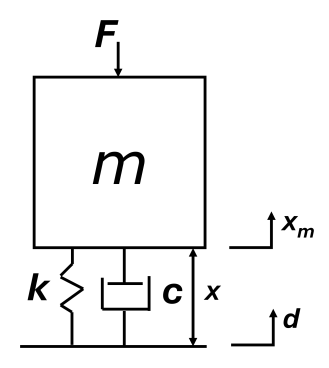


Figure 1: Single degree of freedom mass-spring-damper

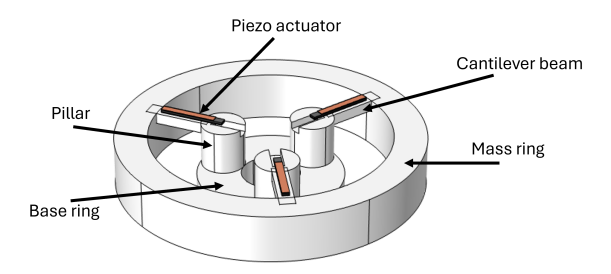


Figure 2: Diagram showing the TVA design showing the main constituent components.

The passive response of the TVA shown in Figure 2 can be tuned according to Equation 3 by either altering the mass of the ring or by modifying either the geometry, L and I, or the Young's modulus, E, from which the cantilever beams are constructed, which has been explored in.³ However, by integrating the piezoelectric actuators into the beams forming the spring elements it is possible to effectively vary the stiffness and damping and thus tune the TVA resonance frequency. The dimensions of the considered TVA were chosen based simply on the dimensions of the available small-scale piezoceramic actuators (Hoerbiger Type 10 piezoceramic actuator⁸). The outer dimensions of the actuator before attaching wires are $9 \times 1 \times 0.5$ mm, and the beams dimensions were thus determined to allow application of the actuators, as given in Table 1. The remaining dimensions of the TVA design were chosen somewhat arbitrarily based on a scaled version of the passive TVAs previously described in Singleton et al.³ As also utilised in Singleton et al.,³ a polyJet multi-material 3D printer (Objet 260 Connex, Stratasys) was used to manufacture the TVA from VeroClear, 9,10 which is an acrylic-like material from that can be used in multi-material inkjet printing. If desired, multiple materials may be used within the same component using the multi-material inkjet printing method, allowing for a greater range of achievable resonance frequencies due to the wider range of material properties available.³ However, for this study, only VeroClear was used for simplicity since the active control system was the area of interest. Figure 3 shows the TVA with the piezoelectric actuators attached.

Mass ring		Beam		Pillar		Base ring	
Outer radius	21	Length	7.5	Radius	2.75	Outer radius	10
Inner radius	16.5	Width	2.1	Height	6	Inner radius	4
Height	6.75	Height	1.5			Height	7.5

Table 1: Dimensions of TVA design in mm.

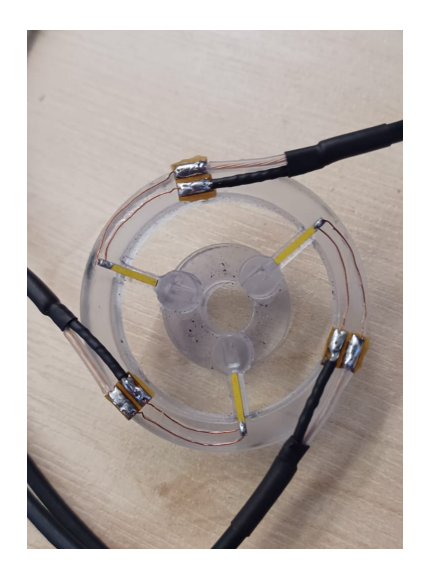


Figure 3: Inkjet printed TVA with piezoelectric actuators attached to the beams.

A. CONTROL STRATEGY

To modify the dynamic response of the TVA the piezoelectric actuators can be driven in a variety of ways to effectively stiffen or soften the beams or modify the damping. The actuators could also potentially be

driven independently to introduce higher-order modes of vibration, or to compensate for either inaccuracies in the manufacturing or changes in the dynamic responses of the three beams over time. However, in this investigation a Single-Input Single-Output (SISO) feedback controller is utilised and all three actuators are driven in parallel. The input to the controller, H, is taken as the average velocity of the mass in the vertical direction measured at the three points where the beams meet the mass ring, \dot{x} , and the output electric potential, u, is applied across all three piezoceramic patches. The controller block diagram is shown in Figure 4, where P represents the passive response of the TVA to base excitation, d, and G represents the secondary path or plant response due to the driven piezoceramic actuators.

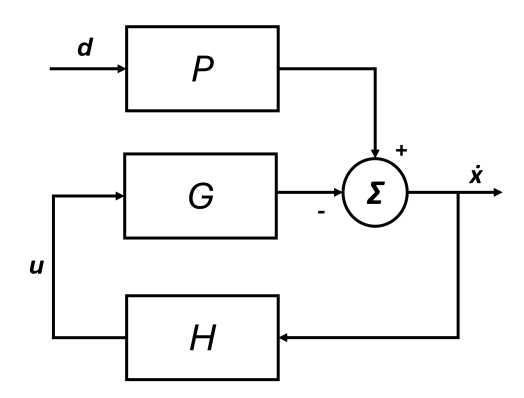


Figure 4: Block diagram showing the feedback controller, H, the passive response of the TVA, P, to base excitation, d, the plant response, G, the control signal, u and the error signal given by the average velocity measured at three points on the mass, \dot{x} .

It has been assumed that the controller, H, is defined as a simple Proportional-Integral-Derivative (PID) controller. Since the error sensor measures the velocity of the mass, the proportional controller gain provides velocity feedback, the integral gain provides displacement feedback, and the derivative gain provides acceleration feedback. It has been shown in the previous simulation-based study into the considered active TVA⁶ that the acceleration and displacement feedback gains are able to modify the resonance frequency of the TVA and the velocity feedback gain is able to control the damping of the TVA. Thus, one or a combination of these gains can be used to shift the effective properties of the TVA to those of the desired mass-spring-damper system. The frequency response of the controller, $H(j\omega)$, for this system configuration can be defined as

$$H(j\omega) = \frac{h_x}{j\omega} + h_{\dot{x}} + j\omega h_{\ddot{x}} \tag{4}$$

where $h_x, h_{\dot{x}}$, and $h_{\ddot{x}}$ are the displacement, velocity, and acceleration feedback gains respectively and ω is the angular frequency. The overall controller response can then be used to calculate the open- and closed-loop responses, as

$$G_{OL}(j\omega) = G(j\omega)H(j\omega) \tag{5}$$

and

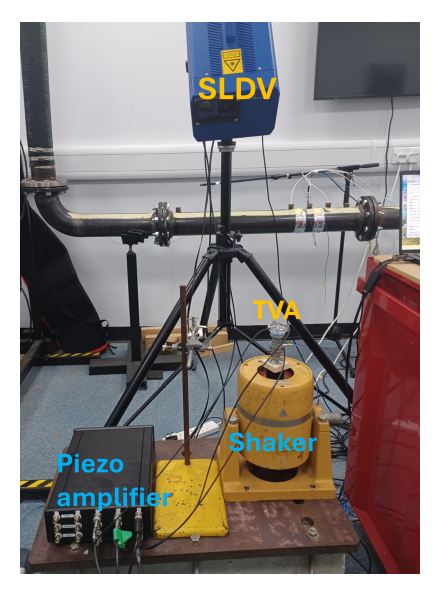
$$G_{CL}(j\omega) = \frac{P(j\omega)}{1 + G(j\omega)H(j\omega)},\tag{6}$$

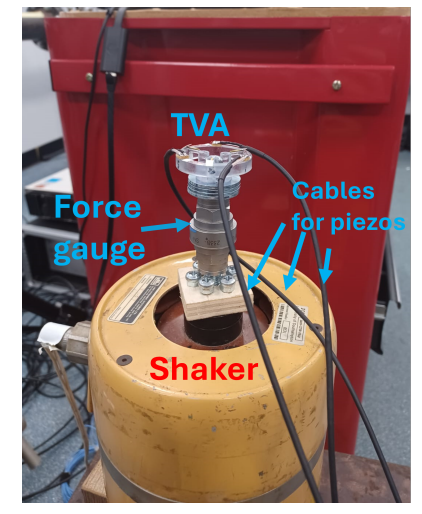
where the open-loop response can be used to assess stability, while the closed-loop response can be used to assess performance giving the ratio between the active and passive responses of the resonator.

3. EXPERIMENTAL SETUP

The response of the implemented TVA shown in Figure 3 has been measured using a Scanning Laser Doppler Vibrometer (SLDV) (Optomet SCAN) when it is excited by either a base excitation or by the piezo-

electric actuators to provide the passive response of the TVA, P, and the plant response, G, respectively. The experimental setup is shown in Figure 5, which shows the TVA mounted to an electromagnetic shaker providing the base excitation via a force gauge. The SLDV was used to measure the velocity at the end points of each of the beams when the TVA was excited by either the shaker or by each of the piezoelectric actuators driven in turn. For each measurement, the respective actuator was driven with a sine sweep between 50 Hz and 2000 Hz and three repeat measurements were averaged to obtain the response of the TVA at each point. This data was then used to calculate the frequency response functions between the input to each of the actuators and the three velocity measurement positions. The passive response of the TVA, P, was then calculated by averaging the responses measured at the three velocity positions; while the plant response, G, was calculated by averaging across the responses measured at the three velocity positions and summing the responses due to the three piezoelectric actuators to represent the condition where all three actuators are driven in phase to realise control. The passive and active measured responses are shown in Figure 6.





(a) Experimental setup including the SLDV and the active TVA mounted to a shaker providing the base (b) Close up image of active TVA with piezo actua-

tors and force gauge

Figure 5: Experimental setup used to measure the response of active TVA to excitation from both base excitation and piezo actuators

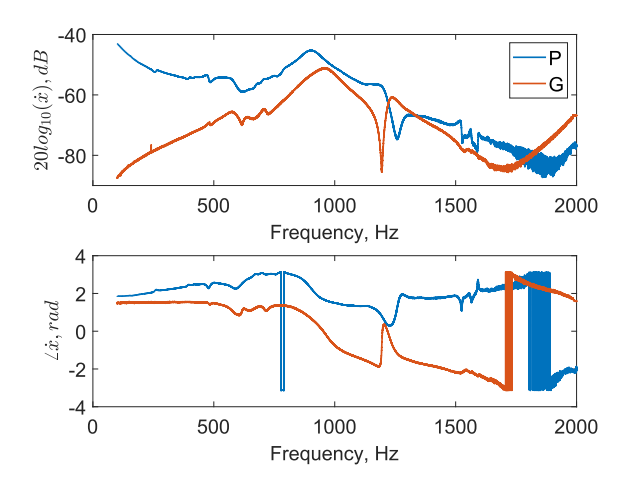


Figure 6: Measured velocity of the primary path, P, and plant response, G, with unity velocity feedback gain across frequency

4. CONTROL PERFORMANCE AND STABILITY ANALYSIS

To investigate the tunability of the active TVA, the responses of the TVA measured according to the method described in Section 3 have been utilised to simulate the performance and stability limits of the feedback controller described by Equation 4. The stability limits have in the first instance been determined for positive and negative velocity, acceleration and displacement feedback gains and then the corresponding change in the resonance frequency, f_0 , and damping ratio, ζ , have been evaluated. Table 2 summarises these results along with the uncontrolled, or passive resonance frequency and damping ratio. From these results it can be seen that the velocity feedback controller modifies the damping of the TVA, with a positive gain resulting in a slight increase in the damping ratio, in addition to an absolute reduction in the peak magnitude, and the maximum stable negative velocity feedback gain resulting in a decrease in the damping by around a factor of 55; it is notable that the positive velocity feedback gain is stable for a large range of gains, however a specific upper limit could not be found. The resonance frequency of the system is also shifted by roughly 4% and 2% respectively for the positive and negative gains. In the case of acceleration feedback, the damping is reduced by a factor of 3 for positive gains and increased by 20% for negative gains, whilst the resonance frequency can be shifted up in frequency by up to around 22% with a negative feedback gain or down in frequency by up to around 10% with a positive feedback gain. Finally, in the case of displacement feedback the largest stable positive gain also gives an increase in the resonance frequency of around 22%, but also results in a decrease of around 34% in the damping; while the largest stable negative displacement feedback gain gives the largest reduction in the tuning frequency, at around 17%, but increase the system damping by around 50%. From these results it can be seen that the considered active arrangement allows a relatively large range of TVA response tuning capability. While combining multiple feedback gains has not been explored here, this will result in some performance trade-off within the presented range of stable tuning capabilities. For example, combining velocity and acceleration feedback may allow both the damping and the tuning frequency to be modified, but is likely to limit the maximum possible degree of tuning in each. Figure 7 shows the Nyquist plots of the three control regimes for positive gains at the stability limits. In the case of velocity control, a gain of 1000 is used such that the Nyquist plot is of a similar scale, however as discussed previously, an upper stable limit could not be identified.

Whilst the results presented in Table 2 demonstrate the limits on active tunability of the resonance frequency and damping, it is also interesting to considered how the feedback controllers influence the response of the TVA away from the resonance frequency. Therefore, Figures 8, 9 and 10 show the closed-loop re-

Gain type	Gain limit	f_0 , Hz	ζ	
Uncontrolled P	n/a	912	0.0609	
$h_{\dot{x}}$	n/a	951*	0.0961*	
$-h_{\dot{x}}$	-360	890	0.0011	
$h_{\ddot{x}}$	17×10^{-2}	816	0.0263	
$-h_{\ddot{x}}$	-17×10^{-2}	1118	0.072	
h_x	90×10^{5}	1112	0.040	
$-h_x$	-90×10^{5}	748	0.0287	

Table 2: Gain limits for stable control and the corresponding tuning frequency and damping ratio for each control regime. *calculated at maximum gain providing calculable values, $h_{\dot x}=1000$

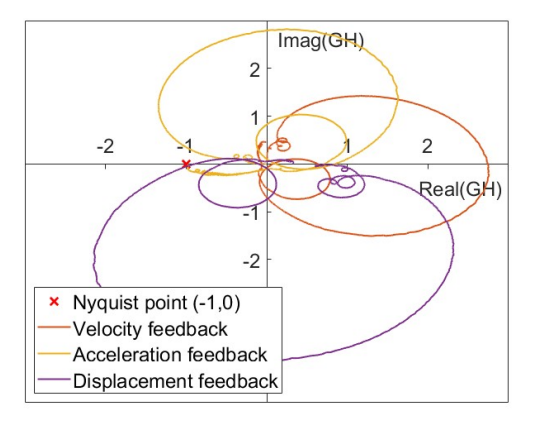


Figure 7: Nyquist plot of three control regimes at stability limits

sponse given in Equation 6 of the TVA for velocity, acceleration and displacement feedback controllers with different levels of both positive and negative gain. In the case of velocity control, shown in Figure 8, a maximum gain of 1000 is used to remain consistent with calculated values in Table 2. From these results it can be seen that by varying the respective gains the TVA response is mostly modified around its first resonance frequency, f_0 , as expected. It can also be seen that the TVA is not behaving as a perfect single degree of freedom system, exhibiting higher order dynamics as shown particularly by the resonance in the responses at around 1.2 kHz. In the case of negative displacement feedback, the rocking mode of the TVA is also excited at around 500 Hz. In comparison to the simulation study reported in,⁶ the range of tuning frequencies and damping factor is significantly lower in the experimental realisation, which can be related to both the additional unmodelled dynamics of the piezoelectric actuators and the higher-order dynamics of the TVA, which were not observed in the modelled system due to it being perfectly excited and perfectly symmetrical. Nevertheless, it can be seen from the results presented here that it is possible to achieve quite effective tuning of the resonance frequency and damping factor using the proposed active TVA.

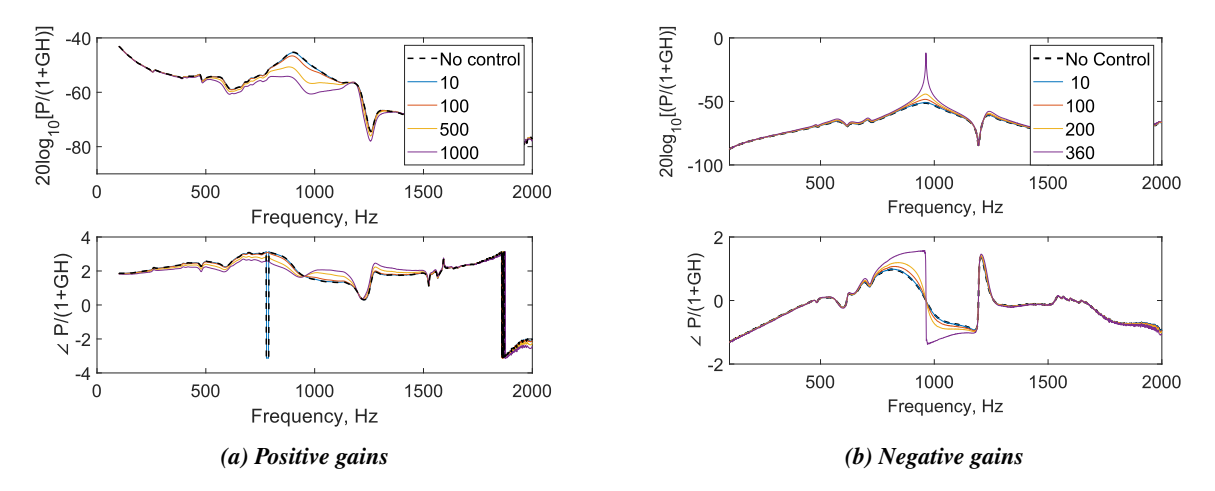


Figure 8: Velocity feedback response for positive and negative gains

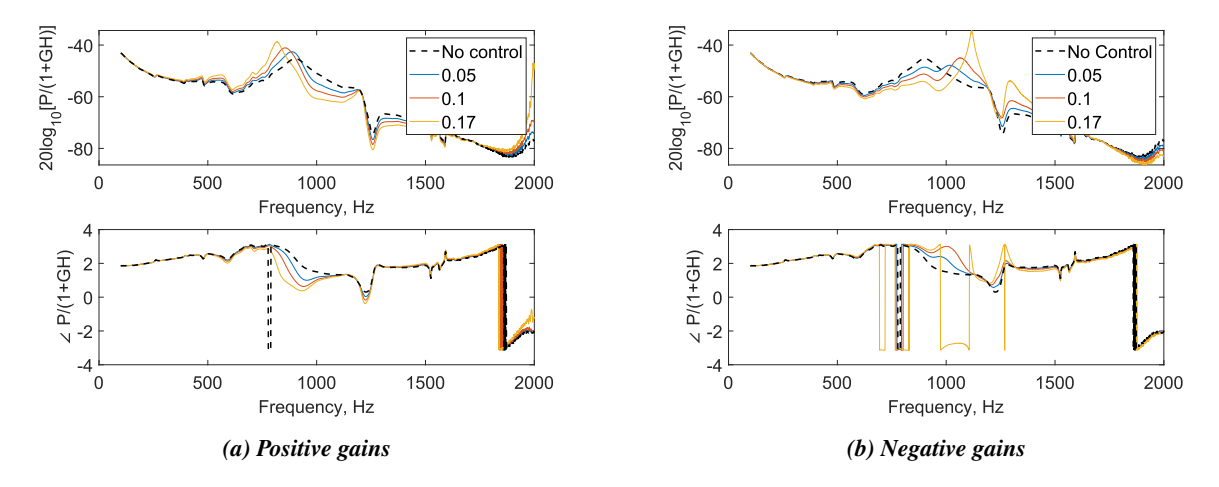


Figure 9: Acceleration feedback response for positive and negative gains

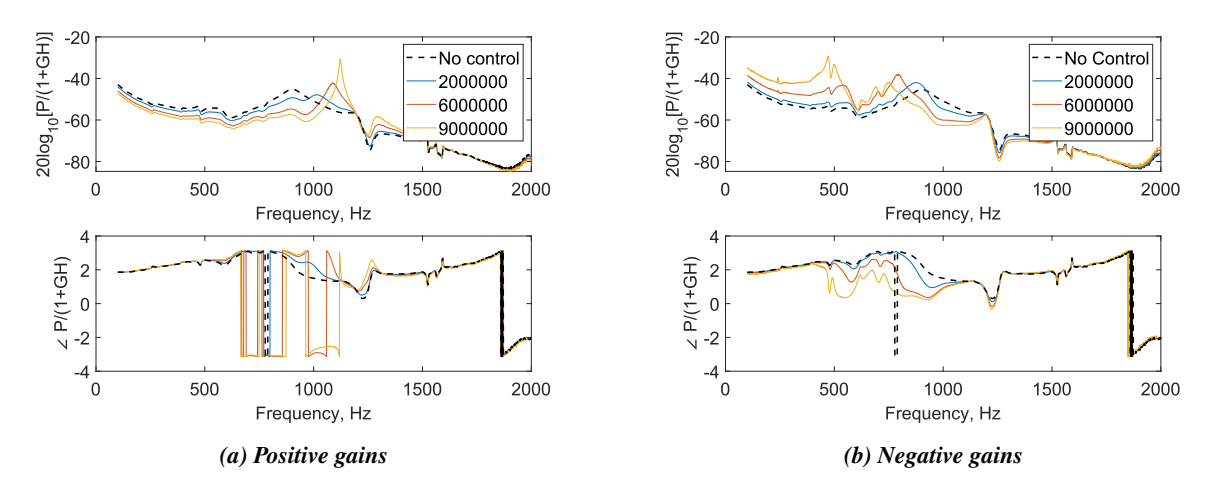


Figure 10: Displacement feedback response for positive and negative gains

5. CONCLUSIONS

This paper has presented and explored the stability and performance of an active TVA. The active TVA is realised by actuating the spring components of a mass-spring-damper like resonator using piezoelectric patch actuators and using velocity, acceleration or displacement feedback control to modify its response. It is assumed that the velocity of the resonator mass is measured at three points and the summation of these three measurements is used to drive the feedback controller. Although in practice physical sensors would need to be integrated into the TVA, this study provides an initial assessment of the potential tunability that can be achieved using the proposed active TVA design.

The presented results demonstrate that velocity feedback control of the active TVA can effectively modify the damping of the system, whilst acceleration and displacement feedback control approaches can modify the resonance frequency. Although the range of tunability is quite significant, it is limited by stability and the higher order dynamics of the TVAs which were not apparent in the previous numerical simulation based study into the proposed active TVA design.⁶ Future work will inevitably explore the integration of a physical sensor into the TVA, as well as the potential of driving the three piezoelectric actuators independently to improve the controllability of the TVA.

REFERENCES

- ¹ J Ormondroyd and J P Den Hartog. The theory of the dynamic vibration absorber. *Trans. ASME*, 50:9–15, 1 1928.
- ² T. Igusa and K. Xu. Vibration control using multiple tuned mass dampers. *Journal of Sound and Vibration*, 175:491–503, 8 1994.
- ³ Lawrence Singleton, Jordan Cheer, Anil Bastola, Christopher Tuck, and Steve Daley. A robust optimised multi-material 3d inkjet printed elastic metamaterial. *Applied Acoustics*, 216:109796, 2024.
- ⁴ Lawrence Singleton, Jordan Cheer, and Steve Daley. A robust optimised shunted electrodynamic metamaterial for multi-mode vibration control. *Journal of Sound and Vibration*, 527:116861, 2022.
- ⁵ Lawrence Singleton and Jordan Cheer. An adaptive electrodynamic metamaterial for the absorption of structural vibration. *Journal of Sound and Vibration*, 582:118414, 2024.

- ⁶ Beth Austin and Jordan Cheer. Active control of a tuned vibration absorber for use in metamaterial applications. *Proceedings of ISMA2024*, September 2024.
- ⁷ Lawrence Singleton, Jordan Cheer, and Stephen Daley. Design of a resonator-based metamaterial for broadband control of transverse cable vibration. *Proceedings of the International Congress on Acoustics*, 2019-Septe(1):5589–5596, 2019.
- ⁸ Hoerbiger. Bending actuators HOERBIGER Motion Control GmbH. https://www.piezoproducts.com/products-solutions/bending-actuators/. [Online; accessed 1-May-2024].
- ⁹ Stratasys. Vero Clear: Rigid Transparent 3D Printing Material. https://www.stratasys.com/en/materials/materials-catalog/polyjet-materials/veroclear/https://www.stratasys.com/materials/search/veroclear, 2020. [Online; accessed 20-June-2022].
- ¹⁰ Stratasys Ltd. PolyJet Materials Data Sheet. https://3dprinting.co.uk/wp-content/uploads/2016/11/Polyjet-Materials-Data-Sheet.pdf, 2016. [Online; accessed 27-March-2023].